

A Time-dependent Numerical Algorithm for the Helmholtz Equation

Daisuke Koyama * (小山 大介)

Department of Computer Science
The University of Electro-Communications
Chofu, Tokyo 182-8585, Japan

1 Introduction

We consider the *controllability method*, which is proposed by Bristeau-Glowinski-Périaux [2], for computing numerical solutions of the exterior problem for the Helmholtz equation. In the controllability method, we need to introduce an artificial boundary in order to reduce the computational domain to a bounded domain, and need to solve, in the bounded computational domain, the wave equation and an elliptic problem iteratively. We first introduce a new *artificial boundary condition* (ABC) for the wave equation, which is suitable for the controllability method. Our ABC is constructed by using the *Dirichlet-to-Neumann* (DtN) operator associated with the Helmholtz equation. We next discuss uniqueness for *semi-discrete solution* of the controllability method in the case when the artificial boundary is a circle. Then we need spectral properties of the DtN operator, which are deduced from some properties of the Hankel functions. We finally present numerical examples, which show that numerical solutions obtained by using our ABC are more accurate than those obtained by using another well-known ABC, and that by using our ABC, accurate numerical solutions are obtained whether the artificial boundary is large or small. These numerical results suggest that by using our ABC and by taking a small artificial boundary, we can reduce the computational costs.

We consider the exterior problem for the Helmholtz equation:

$$\left\{ \begin{array}{ll} -\Delta U - k^2 U = 0 & \text{in } \Omega, \\ U = G & \text{on } \gamma, \\ \lim_{r \rightarrow +\infty} r^{\frac{1}{2}} \left(\frac{\partial U}{\partial r} - ikU \right) = 0 & \text{(outgoing radiation condition).} \end{array} \right. \quad (1)$$

Here k is a positive constant and Ω is an unbounded domain of \mathbf{R}^2 with boundary γ . We assume that $\mathcal{O} = \mathbf{R}^2 \setminus \bar{\Omega}$ is a bounded open set. Further G is a function on γ and $r = |x|$ for $x \in \mathbf{R}^2$. When computing numerical solutions of (1) by using the controllability method, we choose the artificial boundary as follows: $\Gamma_a = \{x \in \mathbf{R}^2 \mid |x| = a\}$, where a is

*e-mail: koyama@im.uec.ac.jp

a positive number such that $\bar{\mathcal{O}} \subset \{x \in \mathbf{R}^2 \mid |x| < a\}$. Then the bounded computational domain becomes as follows: $\Omega_a = \{x \in \Omega \mid |x| < a\}$. In the controllability method, we solve, in the bounded domain Ω_a , the wave equation with an ABC. We propose a new ABC for the wave equation as follows:

$$\frac{\partial u}{\partial n} + \frac{\partial u}{\partial t} = -\mathcal{S}u - iku \quad \text{on } \Gamma_a, \quad (2)$$

where n is the unit normal vector on Γ_a being toward infinity and \mathcal{S} is the *Dirichlet-to-Neumann* (DtN) operator for the Helmholtz equation with the outgoing radiation condition (see Section 2). Bristeau et al. use the following ABC mainly:

$$\frac{\partial u}{\partial n} + \frac{\partial u}{\partial t} = 0 \quad \text{on } \Gamma_a, \quad (3)$$

and do not mention our ABC (2).

Further we discuss the uniqueness for the solution of the semi-discrete problem of the following problem: find $\mathbf{u} = \{u_0, u_1\} \in E_g$ such that

$$\begin{cases} u_{tt} - \Delta u = 0 & \text{in } \Omega_a \times (0, T), \\ u = g & \text{on } \gamma \times (0, T), \\ \frac{\partial u}{\partial n} + \frac{\partial u}{\partial t} = -\mathcal{S}u - iku & \text{on } \Gamma_a \times (0, T), \\ u(x, 0) = u_0(x), \quad u_t(x, 0) = u_1(x) & \text{in } \Omega_a, \\ u(x, T) = u_0(x), \quad u_t(x, T) = u_1(x) & \text{in } \Omega_a, \end{cases} \quad (4)$$

where $T = 2\pi/k$, $g(x, t) = G(x)e^{-ikt}$, $E_g = V_g \times L^2(\Omega_a)$, and

$$V_g = \{v \in H^1(\Omega_a) \mid v = g(0) \text{ on } \gamma\}.$$

Bardos-Rauch [1] discuss uniqueness for the solution of the problem (4) in the case when the ABC is replaced by the ABC (3). However, their analysis is not sufficient to prove the uniqueness for the solution of (4), which is yet to be proved.

2 The DtN operator for the Helmholtz equation

The DtN operator \mathcal{S} can be analytically represented as follows (see Grote-Keller [3]):

$$\mathcal{S}U(a, \theta) = \sum_{n=-\infty}^{\infty} -k \frac{H_n^{(1)'}(ka)}{H_n^{(1)}(ka)} U_n(a) Y_n(\theta), \quad (5)$$

where r, θ are the polar coordinates, $H_n^{(1)}$ are the cylindrical Hankel functions of the first kind of order n , Y_n are the spherical harmonics defined by $Y_n(\theta) = e^{in\theta}/\sqrt{2\pi}$, and $U_n(a) = \int_0^{2\pi} U(a, \theta) Y_n(\theta) d\theta$.

3 Uniqueness for the semi-discrete solution

We discretize the problem (4) by finite element method, and show that the obtained semi-discrete problem has a unique solution under hypotheses described below. For this purpose, we choose a finite dimensional subspace W_h of $H^1(\Omega_a)$, and define $V_h = \{v_h \in W_h \mid v_h = 0 \text{ on } \gamma\}$. Let $\phi_1, \phi_2, \dots, \phi_N$ be a base of V_h , and $\phi_1, \phi_2, \dots, \phi_N, \phi_{N+1}, \dots, \phi_{N'}$ a base of W_h . Then we may assume that $\phi_1, \phi_2, \dots, \phi_{N'}$ are real-valued functions. The semi-discrete problem of the problem (4) can be written as follows: find $\{\xi_0, \eta_0\} \in \mathbf{C}^N \times \mathbf{C}^N$ such that

$$\begin{cases} B \frac{d^2 \xi}{dt^2}(t) + C \frac{d\xi}{dt}(t) + (A + S + ikC) \xi(t) = e^{-ikt} \mathbf{f} & \text{in } (0, T), \\ \xi(0) = \xi_0, \quad \xi_t(0) = \eta_0, \\ \xi(T) = \xi_0, \quad \xi_t(T) = \eta_0, \end{cases} \quad (6)$$

where B, C, A , and S are matrices defined as follows:

$$\begin{aligned} B &= ((\phi_l, \phi_j))_{1 \leq j, l \leq N}, & (u, v) &= \int_{\Omega_a} u \bar{v} dx, \\ C &= (\langle \phi_l, \phi_j \rangle)_{1 \leq j, l \leq N}, & \langle u, v \rangle &= \int_{\Gamma_a} u \bar{v} d\gamma, \\ A &= (a(\phi_l, \phi_j))_{1 \leq j, l \leq N}, & a(u, v) &= \int_{\Omega_a} \nabla u \cdot \nabla \bar{v} dx, \\ S &= (s(\phi_l, \phi_j))_{1 \leq j, l \leq N}, & s(u, v) &= \int_{\Gamma_a} S u \bar{v} d\gamma, \end{aligned}$$

and \mathbf{f} is a vector defined as follows:

$$\begin{aligned} \mathbf{f} &= (f_j)_{1 \leq j \leq N}, \\ f_j &= \sum_{l=N+1}^{N'} \left[k^2(\phi_l, \phi_j) + ik\langle \phi_l, \phi_j \rangle - a(\phi_l, \phi_j) - s(\phi_l, \phi_j) - ik\langle \phi_l, \phi_j \rangle \right] G_j. \end{aligned}$$

Here the non-homogeneous Dirichlet data G is approximated by the following function: $G_h = \sum_{j=N+1}^{N'} G_j \phi_j|_{\gamma}$, where $G_j \in \mathbf{C}$ ($j = N+1, \dots, N'$).

Now we define a square matrix \mathcal{A} of order $2N$ as follows:

$$\mathcal{A} = \begin{bmatrix} O & I \\ -B^{-1}(A + S + ikC) & -B^{-1}C \end{bmatrix},$$

where I is the unit matrix of order N . To show that the problem (6) has a unique solution, we use the following proposition:

Proposition 1 *The problem (6) has a unique solution if and only if*

$$ikl \notin \sigma(\mathcal{A}) \quad \text{for all } l \in \mathbf{Z}, \quad (7)$$

where $\sigma(\mathcal{A})$ is the set of all eigenvalues of the matrix \mathcal{A} .

We show that the problem (6) has a unique solution under two hypotheses described below.

Hypothesis 1 For a positive λ and $u_h \in V_h$, if we have

$$a(u_h, v_h) = \lambda(u_h, v_h) \quad \text{for all } v_h \in V_h,$$

and if we have $u_h = 0$ on Γ_a , then we have $u_h = 0$ in Ω_a .

Hypothesis 1 can be interpreted as follows. The discrete problems of the two eigenvalue problems:

$$\begin{cases} -\Delta u = \lambda u & \text{in } \Omega_a, \\ u = 0 & \text{on } \gamma, \\ \frac{\partial u}{\partial n} = 0 & \text{on } \Gamma_a \end{cases}$$

and

$$\begin{cases} -\Delta u = \lambda u & \text{in } \Omega_a, \\ u = 0 & \text{on } \gamma, \\ u = 0 & \text{on } \Gamma_a \end{cases}$$

have no same eigenpair.

Hypothesis 2 For the wave number k , we take the radius a of the artificial boundary such that

$$\text{Im} \left\{ \frac{H_0^{(1)'}(ka)}{H_0^{(1)}(ka)} \right\} < 2.$$

To explain Hypothesis 2, we here state the following lemma:

Lemma 1 $\text{Im} \left\{ \frac{H_0^{(1)'}(x)}{H_0^{(1)}(x)} \right\}$ is a decreasing function on $(0, \infty)$, and further

$$\begin{aligned} \text{Im} \left\{ \frac{H_0^{(1)'}(x)}{H_0^{(1)}(x)} \right\} &\rightarrow 1 \quad (x \rightarrow +\infty), \\ \text{Im} \left\{ \frac{H_0^{(1)'}(x)}{H_0^{(1)}(x)} \right\} &\rightarrow +\infty \quad (x \rightarrow +0). \end{aligned}$$

By Lemma 1, there exists only one $\alpha > 0$ such that

$$\text{Im} \left\{ \frac{H_0^{(1)'(\alpha)}}{H_0^{(1)}(\alpha)} \right\} = 2.$$

If the radius a of the artificial boundary is taken to satisfy $a > \alpha/k$, then Hypothesis 2 is satisfied. Here we note that $\alpha \approx 0.088426$.

Theorem 1 The problem (6) has a unique solution under Hypotheses 1 and 2.

To prove Theorem 1, we use the following two lemmas:

Lemma 2 For all $x > 0$ and for all $\nu \in \mathbf{R}$, we have

$$\operatorname{Re} \left\{ \frac{H_\nu^{(1)'}(x)}{H_\nu^{(1)}(x)} \right\} < 0.$$

Lemma 3 For all $x > 0$ and for all $\nu, \nu' \in \mathbf{R}$ satisfying $|\nu| > |\nu'|$, we have

$$0 < \operatorname{Im} \left\{ \frac{H_\nu^{(1)'}(x)}{H_\nu^{(1)}(x)} \right\} < \operatorname{Im} \left\{ \frac{H_{\nu'}^{(1)'}(x)}{H_{\nu'}^{(1)}(x)} \right\}.$$

Proof of Theorem 1: Because of Proposition 1, our task is now to show that (7) holds. The proof is by contradiction. Assume that $ikl \in \sigma(\mathcal{A})$ ($l \in \mathbf{Z}$). Then there is $\xi (\neq \mathbf{o}) \in \mathbf{C}^N$ such that

$$\mathcal{A} \begin{bmatrix} \xi \\ \eta \end{bmatrix} = ikl \begin{bmatrix} \xi \\ \eta \end{bmatrix}.$$

Then we have

$$-(kl)^2 B\xi + iklC\xi + (A + S + ikC)\xi = \mathbf{o}. \quad (8)$$

Now we write $\xi = [\xi_1, \xi_2, \dots, \xi_N]^T$ and set $u_h = \sum_{j=1}^N \xi_j \phi_j$. Then (8) is written as follows: for all $v_h \in V_h$,

$$-(kl)^2 (u_h, v_h) + ikl \langle u_h, v_h \rangle + a(u_h, v_h) + s(u_h, v_h) + ik \langle u_h, v_h \rangle = 0. \quad (9)$$

Here if we take $v_h = u_h$ in (9), then we obtain

$$-(kl)^2 (u_h, u_h) + ikl \langle u_h, u_h \rangle + a(u_h, u_h) + s(u_h, u_h) + ik \langle u_h, u_h \rangle = 0.$$

The real part of this identity is:

$$a(u_h, u_h) - (kl)^2 (u_h, u_h) - \frac{k}{a} \sum_{n=-\infty}^{\infty} \operatorname{Re} \left\{ \frac{H_n^{(1)'}(ka)}{H_n^{(1)}(ka)} \right\} \left| \left\langle u_h, \frac{e^{in\theta}}{\sqrt{2\pi}} \right\rangle \right|^2 = 0, \quad (10)$$

and the imaginary part is:

$$\frac{k}{a} \sum_{n=-\infty}^{\infty} \left[l + 1 - \operatorname{Im} \left\{ \frac{H_n^{(1)'}(ka)}{H_n^{(1)}(ka)} \right\} \right] \left| \left\langle u_h, \frac{e^{in\theta}}{\sqrt{2\pi}} \right\rangle \right|^2 = 0. \quad (11)$$

We here consider three different cases.

Case 1: When $l \leq -1$. By Lemma 3,

$$l + 1 - \operatorname{Im} \left\{ \frac{H_n^{(1)'}(ka)}{H_n^{(1)}(ka)} \right\} < 0 \quad \text{for all } n \in \mathbf{Z},$$

and hence, by (11),

$$\left\langle u_h, \frac{e^{in\theta}}{\sqrt{2\pi}} \right\rangle = 0 \quad \text{for all } n \in \mathbf{Z}.$$

This implies

$$u_h = 0 \quad \text{on } \Gamma_a. \quad (12)$$

From this identity and (9), we get

$$a(u_h, v_h) = (kl)^2(u_h, v_h) \quad \text{for all } v_h \in V_h. \quad (13)$$

From (12), (13), and Hypothesis 1, we have $u_h = 0$ on Ω_a , i.e., $\boldsymbol{\xi} = \mathbf{o}$. This contradicts the assumption that $\boldsymbol{\xi} \neq \mathbf{o}$. Therefore we can see $ikl \notin \sigma(\mathcal{A})$.

Case 2: When $l = 0$. By (10), we obtain

$$a(u_h, u_h) - \frac{k}{a} \sum_{n=-\infty}^{\infty} \operatorname{Re} \left\{ \frac{H_n^{(1)'}(ka)}{H_n^{(1)}(ka)} \right\} \left| \left\langle u_h, \frac{e^{in\theta}}{\sqrt{2\pi}} \right\rangle \right|^2 = 0.$$

From this identity and Lemma 2, it follows that $u_h = 0$ in Ω_a . Therefore $0 \notin \sigma(\mathcal{A})$.

Case 3: When $l \geq 1$. By Lemma 3 and Hypothesis 2, we have

$$l + 1 - \operatorname{Im} \left\{ \frac{H_n^{(1)'}(ka)}{H_n^{(1)}(ka)} \right\} > 2 - \operatorname{Im} \left\{ \frac{H_0^{(1)'}(ka)}{H_0^{(1)}(ka)} \right\} > 0 \quad \text{for all } n \in \mathbf{Z}.$$

By the same argument as Case 1, we can conclude that $ikl \notin \sigma(\mathcal{A})$. ■

4 Numerical examples

4.1 Scattering by a disk

We compare the accuracy of numerical solutions obtained by using our ABC (2) and the ABC (3) via numerical experiments. We consider a test problem, where the obstacle $\mathcal{O} = \{x \in \mathbf{R}^2 \mid |x| < 1\}$, the wave number $k = 1$, and the Dirichlet data G is chosen as the exact solution U becomes as follows: $U(r, \theta) = H_1^{(1)}(r) \cos \theta$. We locate the artificial boundary Γ_a at $r = 2$. We use the conforming finite element method using piecewise linear elements. The triangulation has 2176 vertices and 4096 triangles. The length h of each side of every triangle satisfies $\lambda/129 < h < \lambda/54$, where λ is the wave length, i.e., $\lambda = 2\pi/k$. To solve the wave equation numerically, we use explicit second order finite difference centered scheme with the step size $\Delta t = T/200$, where $T = 2\pi/k$. When we use our ABC, we have to truncate the infinite series of (5) at a finite value N . We denote the truncated DtN operator by \mathcal{S}^N . In this test problem, we choose $N = 1$, and then we note that $u = U(r, \theta)e^{-ikt}$ satisfies

$$\frac{\partial u}{\partial n} + \frac{\partial u}{\partial t} = -\mathcal{S}^1 u - iku \quad \text{on } \Gamma_a.$$

We show contour lines of the real part of the exact solution and the numerical solution obtained by the ABC (3) in Figure 1, where solid lines display the numerical solution, and dotted lines the exact solution. We can see that the numerical solution is very different from the exact solution. We show the exact solution and the numerical solution obtained by our ABC in Figure 2, where the numerical solution is exactly coincident with the exact solution. From these figures we can see that numerical solutions obtained by our ABC are more accurate than those obtained by the ABC (3).

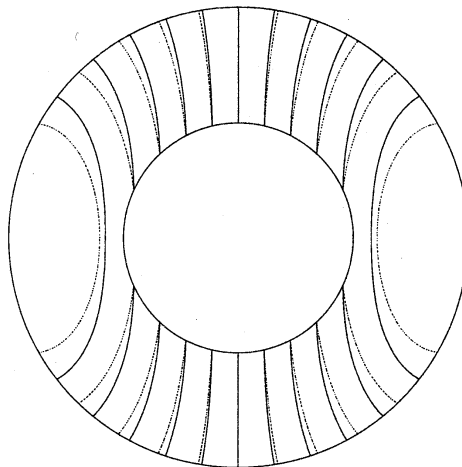


Figure 1: Contour lines of the real part of the exact solution and of the real part of the numerical solution obtained by using the ABC (3).

4.2 Scattering by a Π -shaped open resonator

We compute scattering of an incident plane wave $\exp[ik(x_1 \cos \alpha + x_2 \sin \alpha)]$ by an obstacle, where α is an incident angle. The wave number $k = 8\pi$ and then the wave length $\lambda = 0.25$. The obstacle is a Π -shaped open resonator. The size of its interior rectangle is $4\lambda \times \lambda$, and the thickness of the wall is $\lambda/5$. The incident angle $\alpha = 30^\circ$. First we choose the radius of the artificial boundary $a = 3\lambda$. Then the DtN operator is truncated at $N = 135$, and the triangulation has 42648 vertices and 83808 triangles. The length h of each side of every triangle satisfies $\lambda/51 < h < \lambda/20$. We numerically solve the wave equation by the explicit second order finite difference centered scheme with the step size $\Delta t = T/100$. Next we choose the radius of the artificial boundary $a = 4\lambda$. Then the DtN operator is truncated at $N = 150$, and the triangulation has 77808 vertices and 153888 triangles. The conditions of the mesh size h and the time step size Δt are the same as above. In Figure 3, we display the contour lines of the real part of the numerical solutions in the cases when $a = 3\lambda$ and when $a = 4\lambda$. Figure 3 shows good coincidence of those numerical solutions, and suggests that if we use our ABC, we can get accurate numerical solutions without enlarging radius of the artificial boundary.

5 Acknowledgments

The author would like to thank Professor Takashi Kako for introducing the controllability method to him, Professor Teruo Ushijima for advising him to prove the uniqueness for the semi-discrete solution, and Mr. Yoshio Tsukuda for giving him a software for triangulation, which was used in the numerical experiments of Subsection 4.2.

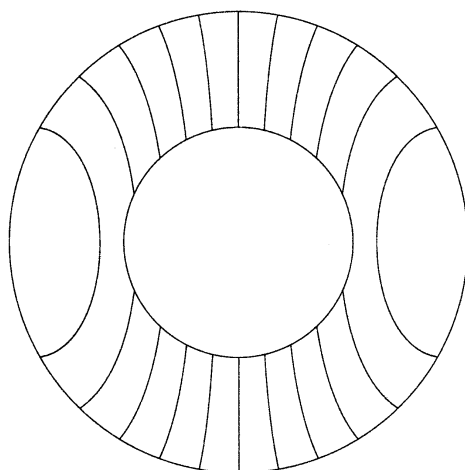


Figure 2: Contour lines of the real part of the exact solution and of the real part of the numerical solution obtained by using our ABC (2).

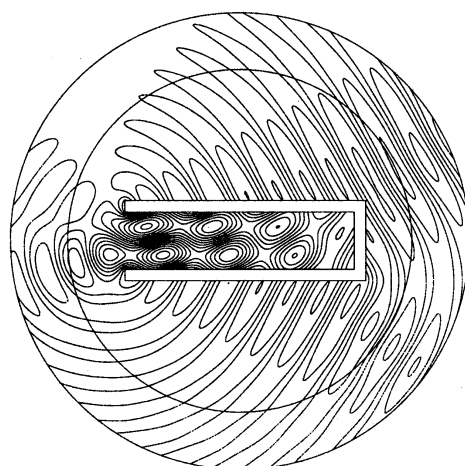


Figure 3: Contour lines of the real part of the numerical solutions in the cases when $a = 3\lambda$ and when $a = 4\lambda$.

References

- [1] C. Bardos and J. Rauch. Variational algorithms for the helmholtz equation using time evolution and artificial boundaries. *Asymptotic Analysis*, 9:101–117, 1994.
- [2] M. O. Bristeau, R. Glowinski, and J. Périaux. Controllability methods for the computation of time-periodic solutions; application to scattering. *J. Comput. Phys.*, 147(2):265–292, 1998.
- [3] M. J. Grote and J. B. Keller. On nonreflecting boundary conditions. *J. Comput. Phys.*, 122(2):231–243, 1995.